Biomechanical effects of rapid maxillary expansion on the craniofacial skeleton, studied by the finite element method

Haluk Işeri*, A. Erman Tekkaya**, Ömer Öztan** and Sadık Bilgiç***

*Department of Orthodontics, School of Dentistry, University of Ankara,
**Department of Mechanical Engineering, Middle East Technical University, Ankara and
***Department of Radiology, Faculty of Medicine, University of Ankara, Turkey

SUMMARY The aim of this study was to evaluate the biomechanical effect of rapid maxillary expansion (RME) on the craniofacial complex by using a three-dimensional finite element model (FEM) of the craniofacial skeleton. The construction of the three-dimensional FEM was based on computer tomography (CT) scans of the skull of a 12-year-old male subject. The CT pictures were digitized and converted to the finite element model by means of a procedure developed for the present study. The final mesh consisted of 2270 thick shell elements with 2120 nodes. The mechanical response in terms of displacement and von Mises stresses was determined by expanding the maxilla up to 5 mm on both sides. Viewed occlusally, the two halves of the maxilla were separated almost in a parallel manner during 1-, 3-, and 5-mm expansions. The greatest widening was observed in the dento-alveolar areas, and gradually decreased through the superior structures. The width of the nasal cavity at the floor of the nose increased markedly. However, the postero-superior part of the nasal cavity was moved slightly medially. No displacement was observed in the parietal, frontal and occipital bones. High stress levels were observed in the canine and molar regions of the maxilla, lateral wall of the inferior nasal cavity, zygomatic and nasal bones, with the highest stress concentration at the pterygoid plates of the sphenoid bone in the region close to the cranial base.

Introduction

Rapid maxillary expansion (RME) procedures have been used over the past century (Angell, 1860), and have been shown to be a valuable aid in the orthodontic treatment of young patients exhibiting maxillary collapse, pseudo-Class III malocclusions, and rhinological and respiratory ailments (Haas, 1970, 1980; Wertz, 1970; Graber and Swain, 1975; Bishara and Staley, 1987).

Different types of RME devices have been used by clinicians and many studies have been conducted to investigate the response of the craniofacial complex. Isaacson *et al.* (1964), and Isaacson and Ingram (1964) measured forces created by a rapid palatal expansion appliance, and reported that a single activation created

between 3 and 10 pounds of force that decayed rapidly at first and continued to decrease slowly. In 1965, Zimring and Isaacson found that maximum forces during RME treatment ranged from 16.6 to 34.8 lb. Gardner and Kronman (1971) showed evidence of distortions in the lambdoid and parietal sutures in rhesus monkeys, as well as in the spheno-occipital synchondrosis. Storey (1973) illustrated that palatal expansion was greater at the alveolar crest and less at the palatal vault, and that the maxillary bones swing laterally with the centre of rotation near the nasofrontal suture. In a study on a human dry skull, Kudlick (1973) concluded that all craniofacial bones directly articulating with the maxilla were displaced, except the sphenoid bone. Wertz and Dreskin (1977) showed that the maxilla

moved downward and usually forward during suture opening, while Timms (1980) showed that the maxilla and palatine bones moved apart, along with the pterygoid processes of the sphenoid bone. Chaconas and Caputo (1982) duplicated a three-dimensional photo-elastic model from a human skull, and reported that the activated RME appliances produced stresses that radiated superiorly along the perpendicular plates of the palatine bone to deeper anatomical structures, such as the lacrimal and nasal bones, as well as the pterygoid plates of the sphenoid.

Although previous studies have provided detailed knowledge regarding the RME technique, the effects of the procedure still remain unclear due to the limited evaluation of the bio-mechanical effects on the internal structures of the craniofacial complex. The finite element method, which has been applied in the mechanical analysis of stresses and strains in the field of engineering, makes it practicable to elucidate the biomechanical state variables such as displacements, strains and stresses induced in living structures by various external forces (Tanne et al., 1989a,b). Therefore, the aim of this study was to evaluate the biomechanical effects of RME on the craniofacial complex by using the FEM as applied to the three-dimensional model of a human skull.

Materials and methods

The finite element analysis was performed on a model of the cranium of a 12-year-old male, with a narrow maxillary base and bilateral posterior crossbite. The subject showed no craniofacial anomaly, and RME treatment was indicated according to the skeletal and dento-alveolar analyses. The geometry of the cranium was obtained by using the computer tomography (CT) technique (Figure 1). The cranium was orientated so that the plane of section passed perpendicular to the orbito-mental plane. CT-images were taken at 5-mm intervals in the parallel horizontal planes. This spacing of CT-images enables a higher geometric accuracy than that used by Tanne et al. (1987; 10 mm) and von Ehler et al. (1975; 30 mm). To verify the model slices in the vertical plane, the geometry-generation phase
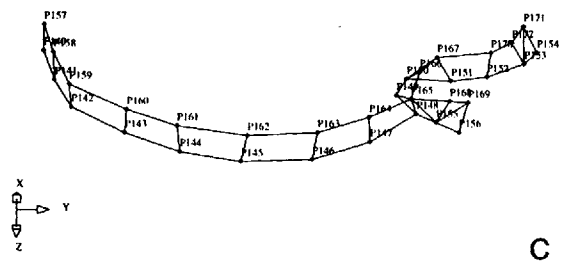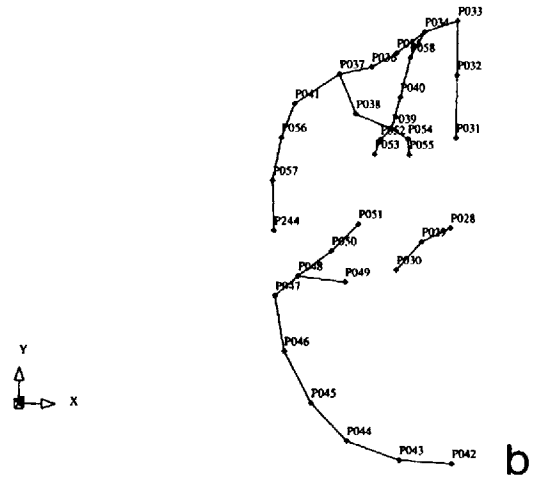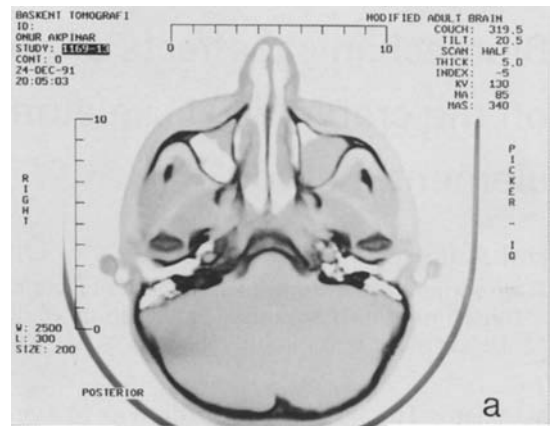

Figure 1 Basic steps of generating the finite element model of the cranium: (a) Sample slices obtained by computer tomography. (b) Geometric lines generated by using geometric points assigned along the midline of the skull bone. (c) Geometric surfaces generated from geometric lines.

was also considered. Hart *et al.* (1992) reported that the positioning error during the scanning of CT-images was approximately 1 mm. This corresponds to an average position error of 0.5 per cent for the present cranium, which is acceptable. The images were scanned and digitized yielding the centrelines between the inner and outer bone boundary as well as the respective bone thickness at typical locations. Along the bone-centreline of each CT-image, geometric points were defined such that geometric lines passing through these points describe the measured bone geometry as close as possible. The straight lines approximated a curved skull section in such a way that approximately 10 straight line segments were used for the representation of a semi-circle. This introduced an error of approximately 0.4 per cent in the arch length of the cranium-model. The geometric points between two neighbouring CT-images were also connected by straight lines forming flat triangular or quadrilateral surfaces between the horizontal slices (Figure 1). The error resulting due to these flat surface between CT-image-planes was in the same range as that for the straight line approximation. Finally, these surfaces were used to generate the finite element mesh as shown in Figure 2. Due to symmetry, only one half of the cranium with respect to the sagittal plane passing between the orbita was considered. The mandible was not modelled. Therefore, it can be concluded that the accuracy of the geometric model of the present study, obtained from CT-images is satisfactory from an engineering point of view.

The finite element computations were conducted using linear shell elements which were able to take into account membrane, i.e. in-plane, deformations as well as bending deformations. Due to these effects, it is necessary to construct the finite element model so that these effects can be considered. The use of standard solid (brick) elements as studied by Tanne *et al.* (1987) cannot describe bending effects, especially if only one element is used across the bone thickness (see Öztan, 1995). In this study, the QUAD4 (warped quadrilateral shell element) and the TRUMP (a triangular plane membrane-bending element) elements of the ASKA element library have been used. Both elements have 6 degrees of
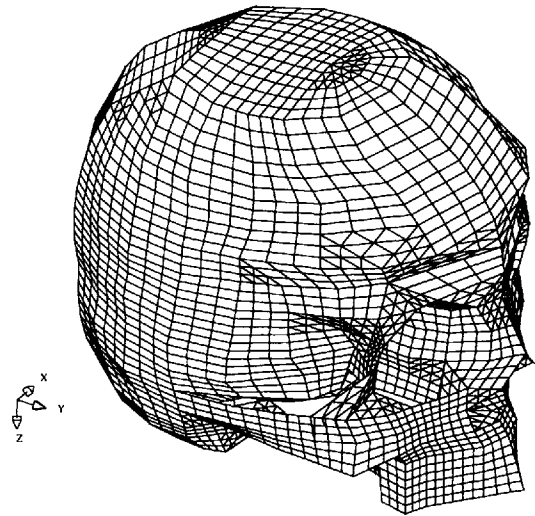

Figure 2 Three-dimensional finite element model of the craniofacial complex. The model consists of 2349 quadrilateral and triangular thick shell elements with 2147 nodes. At each node three translational and three rotational degress of freedom are defined.

freedom (three transitional and three rotational) per node. The thickness of the shell can vary from node to node for both element types. The mesh density of the model was determined by means of a standard convergence study: three meshes were constructed with 1590 (coarse), 5892 (medium), and 12882 (fine) degrees of freedom, respectively. For a critical point, for instance the root of the canine, total displacement values showed a difference of 25 per cent for the coarse mesh as compared with the medium mesh and only 4.7 per cent difference for the medium mesh as compared with the fine mesh. These results indicate that the error due to the topology of the mesh can be estimated as 1 to 2 per cent, since all computations of the RME-study were conducted with the fine mesh.

Solid parts in the interior of the cranium, as well as the maxilla including the teeth, were also modelled with shell elements, which is obviously a crude idealization. For these areas, the thickness of the shell elements was increased, according to the geometric dimensions of the respective part so that an equivalent stiffness effect was simulated.

Table 1 Displacements and stress distributions with 5 mm of RME (x, y and z represent displacements in the transversal, sagittal and vertical planes, respectively).

Structure under analysis	Displacement (mm)			Max. v. Mises stress (kg/mm²)
	x	y	z	
Incisal tip of the maxillary central incisor	5	1.4	1.4	0.72
Cusp of the first molar	5	1.4	0.8	2.09
Maxillary bone at the incisor region	4.99	2.1	1.2	2.29
Maxillary bone at the canine region	4.99	2.1	1.1	18.82
Maxillary bone at the molar region	4.91	2.0	0.4	15.72
Anterior part of the palate	4.9	2.1	1.1	2.09
Palatinal bone	4.8	2.1	0.2	0.96
Inferior part of the pterygoid plate	4.9	1.8	0.04	6.20
Middle part of the pterygoid plate	4.8	2.1	0.01	26.95
Superior part of the pterygoid plate	1.4	1.6	0.7	73.75
Anterior-superior part of the zygomatic bone	3.9	1.6	0.4	41.25
Anterior part of the arcus zygomaticus	3.3	0.7	−0.4	4.28
Posterior part of the arcus zygomaticus	0.6	−0.04	−0.2	0.44
Anterior-inferior part of the outer nasal wall	4.8	2.1	1.1	30.79
Posterior-inferior part of the outer nasal wall	4.8	2.1	0.02	4.95
Posterior-superior part of the outer nasal wall	−0.3	0.2	1.1	12.28
External wall of the orbita	1.6	0.04	−0.3	14.06
Nasal bone	0.3	−1.2	1.1	16.29
Frontal bone	0.03	−0.2	0.5	2.65
Parietal bone	0.0001	−0.05	0.02	0.07
Parse squamosa of the temporal bone	0.1	0.08	−0.4	11.59
Squamo of the occipital bone	−0.002	−0.02	0.02	0.50

The materials in the analysis were assumed to be linearly elastic and isotropic. Three different types of material were considered: compact bone, cancellous bone, and tooth. The elastic properties for these materials are taken from Tanne *et al.* (1987). All sutures were assumed to have the same mechanical properties as the surrounding bone material except at the palatinal bone. The two parts of the palatinal bone which are separated by the vertical plane of symmetry were assumed to be unconnected, so that they move freely in lateral directions with respect to the vertical plane of symmetry.

All points of the cranium lying on the symmetry plane are constrained to have no motion perpendicular to this plane. An exception for this boundary condition were the points at the palatinal bone which were left completely unconstrained. Furthermore, to ensure a unique solution, rigid-body motions were prevented by constraining all degrees of freedom of the nodes along the foramen magnum.

In this study, it was assumed that the two plates of the RME device moved apart by a distance of 2, 6, and 10 mm. Therefore, boundary conditions on the maxillary canine, premolars, and first molar teeth were assigned as the prescribed transversal displacement with magnitudes of 1, 3, and 5 mm, respectively. The RME plates were assumed to be rigid.

Results

Table 1 shows the three-dimensional pattern of displacements and stress distributions observed at 22 anatomical structures located in the craniofacial complex. The findings show that the displacements at the nodes varied linearly for the given displacement boundary conditions due to the RME. This is an expected result since the problem is linear and hence the results vary linearly with the loading. Viewed occlusally, the two halves of the maxillary dento-alveolar complex, basal maxilla, and lateral walls of the
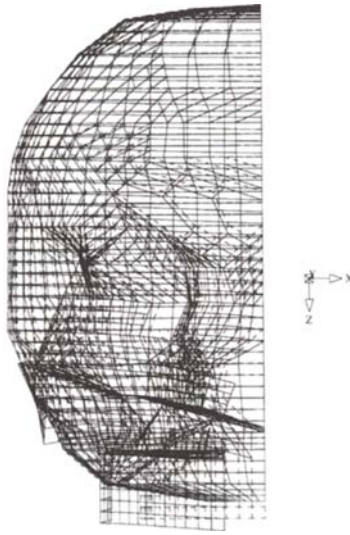
Figure 3 Pattern of computed displacements (– – – – unloaded; —— loaded) of the nasomaxillary complex, with 5 mm of RME. Note that the centre of rotation is located at the frontal bone.

nasal cavity separated almost in a parallel manner. On the other hand, the antero-superior part of the upper nasal cavity separated more than the postero-superior part. No lateral displacement was observed at the temporal, parietal, frontal, sphenoid, and occipital bones. The greatest widening was observed in the dento-alveolar areas, gradually decreasing through the upper structures (Figure 3). The width of the nasal cavity at the floor of the nose increased markedly, while the postero-superior part of the nasal cavity was moved slightly medially. Maxillary bone, maxillary central incisors, and molars were slightly displaced downwards and forwards. The anterior region of the palate and nasal floor descended more than the posterior region. Similarly, the maxillary central incisors displaced downwards more than the maxillary first molars (Figure 4).

The magnitude and distribution of maximum von Mises stresses produced at various areas of the craniofacial complex by the activation of RME device, up to 5 mm on each side, are shown in Table 1 and Figure 5. Highest stress levels were
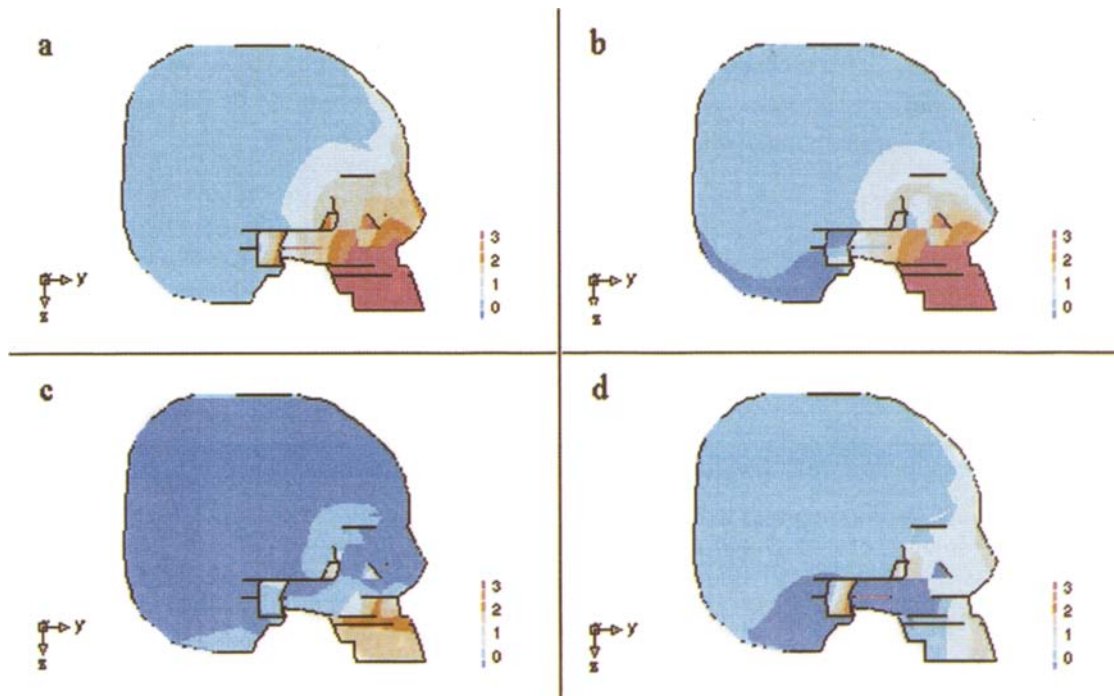
Figure 4   (a) Total, (b) transversal, (c) sagittal, and (d) vertical computed displacement field of the skeletal structures in the craniofacial complex with 5 mm of RME. Red coloured areas represent the structures displaced at least 3 mm.
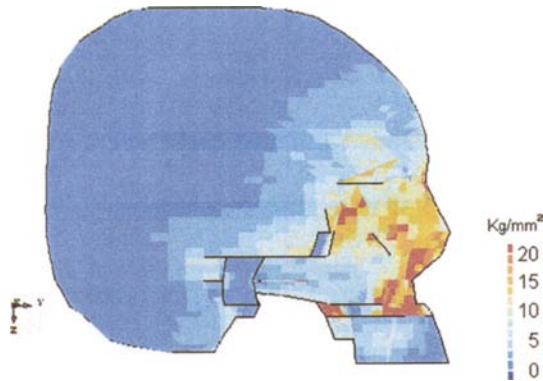
Figure 5 Stress distribution (von Mises; kg/mm²) in the craniofacial complex with 5 mm of RME. Only the maximum values across the thickness are considered. Red coloured areas represent the structures under stress of more than 20 kg/mm².

observed in the pterygoid plate of the sphenoid bone and zygomatic bone. The findings indicated that high stresses produced by the RME are especially located in the superior parts of the pterygoid processes of the sphenoid bone (73.75 kg/mm²). High stress levels were found at the external surface of the zygomatic bone and external wall of the orbita, and decreased along the arcus zygomaticus. In the maxilla, high stresses were observed at the canine and molar regions (18.82 and 15.72 kg/mm², respectively), and were also found around the nasal bone and nasal cavity, especially in the antero-inferior wall of the nasal cavity (30.79 kg/mm²). In the frontal, parietal, temporal and occipital bones, RME produced stress levels ranging from 0.07 to 11.59 kg/mm².

Discussion

Several studies have been conducted to investigate histologically, morphologically and biomechanically the response of the craniofacial complex to RME. During orthodontic treatment, the craniofacial skeleton is subjected to complex loading and it would be difficult to assess the mechanical reaction of the craniofacial bones to complex loading in three-dimensional space by using conventional methods, namely, strain gauge (Tanne *et al.*, 1985), photoelastic (Chaconas

and Caputo, 1982) or holographic (Pavlin and Vukicevic, 1984) techniques. In addition, it has been suggested that by using roentgenographic cephalometric methods (RCM) only anecdotal observations are possible and RCMs are incapable of correctly depicting, in detail, time-related changes or changes in location of biological shapes (Moyers and Bookstein, 1979). The three-dimensional finite element model used in the present study provides the freedom to simulate orthodontic force systems applied clinically and allows analysis of the response of the craniofacial skeleton to the orthodontic loads in three-dimensional space. The point of application, magnitude, and direction of a force may easily be varied to simulate the clinical situation. Thus, FEM would be an effective approach in the investigation of the biomechanical behaviour of the craniofacial skeleton in three dimensions.

Analytical results of the FEM are highly dependent on the models developed, so they have to be constructed to be equivalent to real objects in various aspects. The finite element computations provide results which include errors as a consequence of the geometry idealization, material characteristic properties, and boundary conditions. Furthermore, the results are valid only for a single specific 12-year-old male. From a structural engineering analyst's point of view, geometry idealization, material data selection, and assignment of boundary conditions of the present analysis are sound as long as the mechanical consequences of RME are investigated. In other words, the results are qualitatively valid even if, for instance, the Young's modulus or the geometry of the skull are an assumption. However, it would be a pitfall to believe that the supplied numerical values are applicable quantitatively even for this specific case study. The situation gets even worse if a generalization of the results is attempted for other patients. In this context, it is worth mentioning that comparative computations with the present cranium have been conducted using the material and loading data of Tanne *et al.* (1987) and, respectively, of von Ehler *et al.* (1975), who used different skull geometries than the present 12-year-old male. Furthermore, the finite element models used in these three studies are qualitatively and quantitatively distinct.

Interestingly, the results obtained with the present model supplied qualitatively similar results when compared with both Tanne *et al.* (1987) and von Ehler *et al.* (1975). For example, Figure 6a shows the maximum principal stress distribution at the level of the superior ridge of the nasal fossa for common nodal points as obtained by the present skull geometry with the loading and material data and results of Tanne *et al.* (1987), and Figure 6b depicts the horizontal displacements at the apex of the first molar as a function of varying force directions. Although there are quantitative differences, qualitatively, the mechanical response is predicted in the same manner, which is a positive indication for the validity of the qualitative conclusions.

Details of FEMs developed using CT scanning have been previously published (Hart *et al.*, 1992; Korioth *et al.*, 1992). Hart *et al.* (1992) used two different methods to obtain the digitized description of mandibular geometry, and suggested that the non-destructive method based on CT scans proved advantageous to a technique that involved embedding the mandible in a plastic resin and cutting serial sections.

The subject in this study was a 12-year-old male, with a narrow maxillary base and bilateral posterior crossbite. He showed no craniofacial anomaly. According to the cephalometric and dental cast analyses, RME treatment was indicated. Different types of maxillary expansion devices have been used by clinicians for rapid maxillary expansion of the mid-palatal suture, and certain advantages of the bandless, indirectly fabricated acrylic bonded RME appliances with occlusal coverage are reported (Howe, 1982; Spolyar, 1984; Alpern and Yorusko, 1987; Memikoğlu *et al.*, 1994, 1997; Memikoğlu and Işeri, 1997). The appliance model used in the present study simulates the same boundary conditions (predescribed displacements) as the acrylic bonded RME device.

The greatest widening was observed in the dento-alveolar structures, with the expansion effect gradually decreasing through the upper structures. Viewed anteriorly, the nasomaxillary complex rotated with the fulcrum of rotation around the upper border of the orbita. Previous studies have shown that the maxillary suture
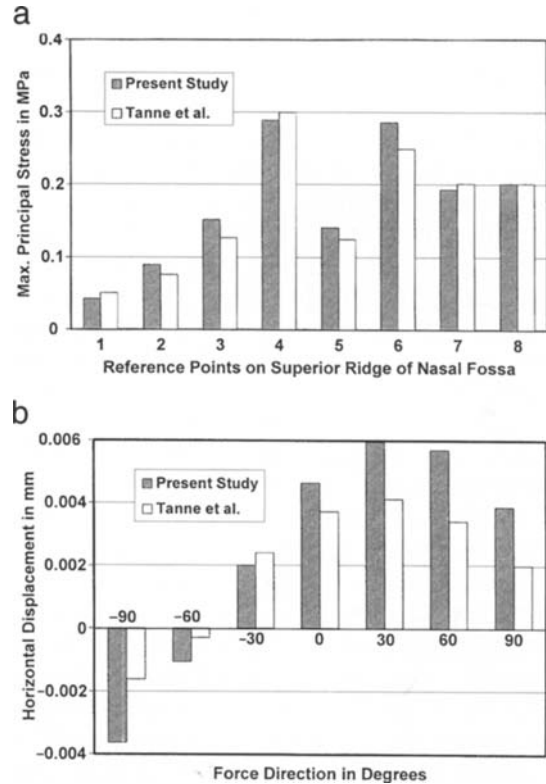

Figure 6 Comparison between computations by Tanne *et al.* (1987) and present study. In both computations the same material and loading data are used, whereas the geometry of the cranium is distinct. The direction of the force was backward with a magnitude of 10 N, and applied to the maxillary first molar parallel to the functional occlusal plane. (a) Maximum principal stresses for the level of superior ridge of nasal fossa. (b) Horizontal displacements at the apex of the first molar as a function of the force direction.

is found to separate supero-inferiorly in a non-parallel manner, the separation being pyramidal in shape with the base of the pyramid located at the oral side of the bone, and the centre of rotation located near the fronto-maxillary suture (Krebs, 1959, 1964; Haas, 1961, 1970; Wertz, 1968, 1970; Memikoğlu *et al.*, 1994, 1997). By using implants, Hicks (1978) reported that maxillae were found to tip between –1 to +8 degrees relative to each other. In a previous study, Memikoğlu *et al.* (1994) found that the basal maxillary angle changed with a mean of 3 degrees with bonded RME. Thus, the findings of the previous studies regarding the transversal rotation of the maxilla

with RME are confirmed by the computational results of the present study.

Fried (1971) and Haas (1961, 1965) reported that the palatine processes of the maxilla were lowered as a result of the outward tilting of the maxillary halves. On the other hand, Davis and Kronman (1969) noted that the palatal dome remained at its original height. The analytical results of the present study support the findings of Fried (1971) and Haas (1961, 1965), and also indicate that the anterior region of the palatal processes lowered more than the posterior region. The maxillary central incisors and molars showed some extrusion, which was also demonstrated in previous studies (Byrum, 1971; Hicks, 1978; Memikoğlu et al., 1994, 1997).

Many investigators have pointed out that RME is not only limited to the palate but also causes dramatic changes in the craniofacial structures. Kudlick (1973), in a study on a human dry skull that simulated the in vivo response of RME suggested that all craniofacial bones directly articulating with the maxilla were displaced except the sphenoid bone. Gardner and Kronman (1971), in a study of RME in rhesus monkeys found that the lambdoid, parietal, and mid-sagittal sutures of the cranium showed evidence of disorientation, and in one animal these sutures split 1.5 mm. However, no displacement of parietal, frontal, and occipital bones was observed in the present study.

Various investigators have shown that there is an increase in the width of the nasal cavity following expansion, particularly at the floor of the nose (Haas, 1961, 1965, 1970; Wertz, 1970; Memikoğlu et al., 1994). As the maxillae separate, the outer walls of the nasal cavity move laterally. The nasal cavity width gain averaged 1.9 mm, but can widen as much as 8–10 mm at the level of the inferior turbinates (Gray, 1975), while the more superior areas might move laterally (Pavlin and Vukicevic, 1984). In 1968, Wertz confirmed the advantage of rapid palatal expansion in improving nasal air flow in patients with stenosis of the nasal airway, and reported the greatest benefit where the stenosis was primarily in the anterior-inferior region, while those patients with stenosis in the posterior-superior part of the nasal airway did not benefit

from palatal expansion. The numerical results of the present study demonstrate that the width of the nasal cavity at the floor of the nose increased markedly compared with the superior parts, and the posterior-superior region was moved slightly medially (–0.3 mm) as previously speculated by Pavlin and Vukicevik (1984).

Bishara and Staley (1987) suggest that the main resistance to mid-palatal suture opening is probably not in the suture itself, but in the surrounding structures in the sphenoid and zygomatic bones. In fact, the highest stress levels in this investigation were observed at the sphenoid and zygomatic bones, particularly at the superior parts of the pterygoid plates of the sphenoid bone, and anterior part of the zygomatic bone (Table 1). In skull material, it has been shown that the heavy interdigitation of the osseous surfaces between the palatine bone and the maxilla, and the pterygoid processes of sphenoid bone makes disarticulation difficult in the late juvenile and early adolescent periods (Melsen and Melsen, 1982). Wertz (1970) mentioned that the confining effect of the pterygoid plates of the sphenoid bone minimizes dramatically the ability of the palatine bones to separate at the mid-sagittal plane. Timms (1980) suggests that the pterygoid plates can bend only to a limited extent as pressure is applied to them, and their resistance to bending increases in the parts closer to the cranial base. On the other hand, the analytical results obtained in the present study show that the inferior and middle parts of the pterygoid plates markedly displace or bend laterally, and high stresses develop particularly in the region close to the cranial base where the plates are more rigid. The deep anatomical effect of these orthopaedic appliances was also observed by the high stress levels in the areas of the zygomatic and maxillary bone, in the maxillary molar area, zygomatic process and external wall of the orbita. Therefore, phenomena, such as dizziness and a feeling of heavy pressure on the bridge of the nose, under the eyes and generally throughout the face, reported during RME (Zimring and Isaacson, 1965), could be due to the forces in the nasal, sphenoid and zygomatic areas which are produced by activation of the RME appliances.

Conclusions

The above findings indicate that RME not only produces an expansion force at the intermaxillary suture, but also high forces on various structures in the craniofacial complex. Rapid displacement or deformation of the facial bones results in a marked amount of relapse in the long term, while relatively slower expansion of the maxilla would probably produce less tissue resistance in the nasomaxillary structures. Therefore, slow maxillary expansion followed by RME, immediately after the separation of the mid-palatal suture, would stimulate the adaptation processes in the nasomaxillary structures, and also would result in reduction of relapse in the post-retention period.

Future studies will aim to model the suture as a viscoelastic material with hardening properties, and experimental studies will be necessary to determine the material properties of the sutural structures under growing conditions.

Address for correspondence

Haluk Işeri
Ankara Üniversitesi
Diş Hekimliği Fakültesi
Ortodonti Anabilim Dalı
Beşevler
Ankara 06500
Turkey

References

Alpern M C, Yurosko J J 1987 Rapid palatal expansion in adults with and without surgery. Angle Orthodontist 57: 245–263

Angell E C 1860 Treatment of irregularities of the permanent or adult teeth. Dental Cosmos 1: 540–544

Bishara S E, Staley R N 1987 Maxillary expansion: clinical implications. American Journal of Orthodontics and Dentofacial Orthopedics 91: 3–14

Byrum A G Jr 1971 Evaluation of anterior-posterior and vertical skeletal changes in rapid palatal expansion cases as studied by lateral cephalograms. American Journal of Orthodontics 60: 419 (Abstract)

Chaconas S J, Caputo A A 1982 Observation of orthopedic force distribution produced by maxillary orthodontic appliances. American Journal of Orthodontics 82: 492–501

Davis M W, Kronman J H 1969 Anatomical changes induced by splitting the mid-palatal suture. Angle Orthodontist 39: 126–132

Fried K H 1971 Palate-tongue reliability. Angle Orthodontist 61: 308–323

Gardner G E, Kronman J H 1971 Cranioskeletal displacements caused by rapid palatal expansion in the rhesus monkey. American Journal of Orthodontics 59: 146–155

Graber T M, Swain B F (eds) 1975 Dentofacial orthopedics. In: Current orthodontic concepts and techniques. Vol. 1. W B Saunders Company, Philadelphia

Gray L P 1975 Results of 310 cases of rapid maxillary expansion selected for medical reasons. Journal of Laryngology and Otolaryngology 89: 601–614

Haas A J 1961 Rapid expansion of the maxillary dental arch and nasal cavity by opening the mid-palatal suture. Angle Orthodontist 31: 73–90

Haas A J 1965 The treatment of maxillary deficiency by opening the mid-palatal suture. Angle Orthodontist 35: 200–217

Haas A J 1970 Just the beginning of dentofacial orthopedics. American Journal of Orthodontics 57: 219–255

Haas A J 1980 Long term post-treatment evaluation of rapid palatal expansion. Angle Orthodontist 50: 189–217

Hart R T, Hennebel V V, Thongpreda N, Van Buskirk W C, Anderson R C 1992 Modeling the biomechanics of the mandible: a three-dimensional finite element study. Journal of Biomechanics 25: 261–286

Hicks E P 1978 Slow maxillary expansion: A clinical study of the skeletal vs. dental response to low magnitude force. American Journal of Orthodontists 73: 121–141

Howe R P 1982 A case involving the use of an acrylic-lined bondable palatal expansion appliance. American Journal of Orthodontics 82: 464–468

Isaacson R J, Ingram A H 1964 Forces produced by rapid maxillary expansion. Part II. Forces present during treatment. Angle Orthodontist 34: 261–269

Isaacson R J, Wood L J, Ingram A H 1964 Forces produced by rapid maxillary expansion. Design of the force measuring system. Angle Orthodontist 34: 256–260

Korioth T W P, Romilly D P, Hannam A G 1992 Three-dimensional finite element stress analysis of the dentate human mandible. American Journal of Physical Anthropology 88: 69–96

Krebs A A 1959 Expansion of mid palatal suture studied by means of metallic implants. Acta Odontologica Scandinavica 17: 491–501

Krebs A A 1964 Rapid expansion of mid palatal suture by fixed appliance. An implant study over a 7 year period. Transactions of European Orthodontic Society, pp. 141–142

Kudlick E M 1973 A study utilizing direct human skulls as models to determine how bones of the craniofacial complex are displaced under the influence of mid-palatal expansion (Master's thesis). Fairleigh Dickinson University, Rutherford, New Jersey

Melsen B, Melsen F 1982 The postnatal development of the palatomaxillary region studied on human autopsy material. American Journal of Orthodontics 82: 329–342

Memikoğlu T U, Işeri H, Uysal M E 1994 Three dimensional dentofacial changes with bonded and banded rapid maxillary expansion appliances. European Journal of Orthodontics 16: 342 (Abstract)

Memikoğlu T U, Işeri H, Uysal M 1997 Comparison of dentofacial changes with rigid acrylic bonded and Haas type banded rapid maxillary expansion devices. Turkish Journal of Orthodontics 10: 255–264

Memikoğlu T U, Işeri H 1997 Nonextraction treatment with rigid acrylic bonded rapid maxillary expander. Journal of Clinical Orthodontics 31: 113–118

Moyers R E, Bookstein F L 1979 The inappropriateness of conventional cephalometrics. American Journal of Orthodontics 75: 599–617

Öztan Ö 1995 Deformations and stress states in a human skull exposed to orthodontic forces (Master of Science thesis). Middle East Technical University, Turkey

Pavlin D, Vukicevic D 1984 Mechanical reactions of facial skeleton to maxillary expansion determined by laser holography. American Journal of Orthodontics 85: 498–507

Spolyar J L 1984 The design, fabrication, and use of a full coverage bonded rapid maxillary expansion appliance. American Journal of Orthodontics 86: 136–145

Storey E 1973 Tissue response in the movement of bones. American Journal of Orthodontics 64: 229–247

Tanne K, Miyasaka J, Yamagata Y, Sakuda M, Burstone C J 1985 Biomechanical changes in the craniofacial skeleton by the rapid expansion appliance. Journal of Osaka University Dental Society 30: 345–356

Tanne K et al. 1987 Three-dimensional model of the human craniofacial skeleton: method and preliminary results using finite element analysis. Journal of Biomedical Engineering 10: 246–252

Tanne K, Hiraga J, Kuniaki K, Yoshiaki Y, Sakudo M 1989a Biomechanical effect of anteriorly directed extraoral forces on the craniofacial complex: A study using the finite element method. American Journal of Orthodontics and Dentofacial Orthopedics 95: 200–207

Tanne K, Hiraga J, Sakuda M 1989b Effects of directions of maxillary protraction forces on biomechanical changes in craniofacial complex. European Journal of Orthodontics 11: 382–391

Timms D J 1980 A study of basal movement with rapid maxillary expansion. American Journal of Orthodontics 77: 500–507

von Ehler E, Trinks R D, Schmitz K P, Pfau H 1975 Zur Berechnung von Verformungen der durch Punktlast beanspruchten menschlichen Schaedelkalotte unter Verwendung der Methode der Finiten Elemente. Wissenschaftliche Zeitschrift der Universitaet Rostock 24: 969–979

Wertz R A 1968 Changes in nasal airflow incident to rapid maxillary expansion. Angle Orthodontist 38: 1–11

Wertz R A 1970 Skeletal and dental changes accompanying rapid mid-palatal suture opening. American Journal of Orthodontics 58: 41–66

Wertz R, Dreskin M 1977 Midpalatal suture opening: A normative study. American Journal of Orthodontics 71: 367–381

Zimring J F, Isaacson R J 1965 Forces produced by rapid maxillary expansion. III. Forces present during retention. Angle Orthodontist 35: 178–186